Proceedings of HT-FED04
2004 ASME Heat Transfer/Fluids Engineering Summer Conference
July 11-15, 2004, Charlotte, North Carolina USA

HT-FED04-56013

MODELLING OF SLURRY-HANDLING PIPING ELEMENT UNDER INTERFERENCE CONDITIONS

Dr. Prem Chand *
Professor
Department of Mechanical Engineering
Indian Institute of Technology
Kharagpur, 721302
India

Dr. K. Govinda Rajulu
Professor of Mechanical Engineering
JNT University, Hyderabad 500072, India.
Y. Krishna Reddy
Asso. Professor, Department of Mechanical Engineering.
CBIT, Gandipet, Hyderabad, India.

Keywords:- Jet Pump, Hydraulic Transport, Pipeline Transportation, Slurry Pumping, Interference.

ABSTRACT

The paper presents a new approach to predict the two-phase performance of jet-pumps under interference conditions. We limit our study mainly to diffuser and transport regions of the jet pump. The five essential pre-requisites which form the backbone of our approach are a fairly generalized and accurate approach to (i) solid-fluid interaction, (ii) particle diffusion under generalized flow field, (iii) friction factor-Reynolds number equation, (iv) solid-fluid flow through ducts and (v) mixing of primary and secondary jets using the approach of Wang et al. [1] based on boundary layer concept. The extensive experimental data of several research workers along with fresh data generated on specially designed test-rig support the new approach.

NOMENCLATURE

A	Sectional area	(m^2)
C	Concentration	(-)
C_d	Drag coefficient	(-)
c	Local concentration	(-)
$\overline{c}$	Mean concentration	(-)
c_b	Concentration at the bottom wall	(-)
c_p	Pressure coefficient	(-)
D	Pipe diameter	(m)
d	Particle diameter	(m)
d_n	Nozzle diameter	(m)
d_t	Throat diameter	(m)
e	Pipe roughness	(m)
f	Friction factor	(-)
g	Acceleration due to gravity	$(\frac{m}{s^2})$
$K_1 - K_6$	Coefficients	(-)
l	Length	(m)
m	Mass of a single particle	(kg)
m_r	Mixture ratio = $\frac{\rho_q \lambda}{\rho_s(1-\lambda)}$	(-)
N	Particle number density	$(\frac{1}{m^3})$
n	Exponent in power law equation	(-)
P/p	Pressure	(Pa)
R/r	Radius	(m)
Re	Reynolds number = $\frac{Du}{\nu}$	(-)
T	Particle terminal velocity	$(\frac{m}{s})$
u	Fluid velocity	$(\frac{m}{s})$
u^*	Shear velocity	$(\frac{m}{s})$
u_{LX}	Slip velocity	$(\frac{m}{s})$
V	Average velocity	$(\frac{m}{s})$
V_s	Secondary velocity	$(\frac{m}{s})$
W	Mass flow rate	$(\frac{kg}{s})$
x	Distance from throat entry	(m)
$\hat{x}$	(+) when UP and (-) when DOWN	(-)
y	Distance from the bottom wall	(m)

*Address all correspondence to this author.

Greek Symbols

δ	Boundary layer growth	(m)
θ	Azimuthal angle to define y	(^{0})
ϑ	Pipe slope	(^{0})
λ	Loading Ratio	(-)
μ	Friction coefficient	(-)
ν	Kinematic viscosity	$\frac{m^2}{s}$
ρ	Density	($\frac{kg}{m^3}$)
ψ	Sphericity	(-)

Subscripts

bl	Blasius
c	Centerline
exp	Experiment
g	Gas/Fluid
l	Laminar
n	Nozzle
N	Newtononian region
p	Particle/Primary flow region
s	Solid/Secondary flow region
sh	Shih
sj	Swamee and Jain
t	Throat

1 INTRODUCTION

Jet pumps have been used in several forms and in diverse applications such as in mining, coal and cinder transport in power plants, marine unloading of pulverized coal, chemical plant circulating systems in dredging, deep-sea mining, aircraft fuel pumping, boiling water re-circulating system in nuclear reactors etc. They have drawn the attention of a large number of researchers like Cunningham [2], Reddy et al. [3], and Ng [4] to name a few. However, a systematic treatment of two-phase flow under generalized flow conditions and the resulting performance particularly when the pump is subjected to interactions is absent. Many researchers even proposed generalized correlations using experimental data generated on set-ups where interference conditions clearly prevailed. It is obvious that such correlations are test rig specific, as dynamic similarity is not possible between set-ups affected differently due to different degrees of interference even for single phase flow as could be seen through several graphs and tables of Idelchik [5], and Miller [6].

2 PREREQUISITES TO THE NEW APPROACH

Thorough study of jet pumps handling solids requires a well established procedure to predict two phase pressure distribution along flow lines which in turn requires as a pre-requisite, admitting into the formalism, the following five aspects.

2.1 Solid-Fluid Interaction

The best source material to deal with solid fluid interaction is reported by Brown [7]. In one of our papers [8], we accepted Cd-Re_p relationship for particle of sphericity ψ to be of the same form as for the spherical particles [9], as shown in Eq. 1.

$$C_d = \begin{cases} \frac{K_l}{Re_p} & Re_p < Re_{pl} \\ \frac{K_l}{Re_p} + \frac{K}{Re^{\xi}} & Re_{pl} \le Re \le Re_{pN} \\ C_{dN} & Re_{pl} > Re_{pN} \end{cases} \quad (1)$$

In each of the three regions- laminar, transition and Newtonian, there are two parameters (K_l, Re_{pl}), (K,ξ) and (Re_{pN},Cd_N) respectively to characterize the Cd-Re_p plots of Brown [7]. The numerical values of the six parameters for different sphericity are listed in Table 1. After interpolating the six parameters corresponding to the required sphericity, the parameters (K_l, Re_{pl}), (K,ξ) and (Re_{pN},Cd_N) can be obtained. They can then be used to find the drag coefficient for the particle at any Reynolds number using Eq. 1.

Table 1. PARAMETER ARRAY.

ψ	0.125	0.220	0.600	0.806	1
Re_{pl}	0.1	0.14	0.3	0.4	0.5
K_l	77	74	59	42	24
K	24.75	23.5	18	12.5	3.4
ξ	0.100	0.175	0.260	0.295	0.306
Re_{pN}	20	350	790	950	1000
C_{d_N}	20	8	3	1.5	0.4

Using this method for spherical particles, the agreement between the predicted drag coefficient and the experimental values is found to be within 9% in the Reynolds number range up to 3000. On increasing the range of Reynolds number to 3,50,000, the maximum, minimum, average and RMS errors expressed as percentages are 12.61, -13.19, -1.37 and 6.47 respectively.

2.2 Mass Transfer Parameter

In an earlier study [9], one dimensional mass transport equation was used to obtain the particle number density distribution at a section. This assumed the particle diffusion coefficient to be equal to the linear momentum diffusion coefficient as reported by Taylor [10] and equals $10.1u^*R$. Where shear velocity u* equals

$(u\frac{\sqrt{f}}{2\sqrt{2}})$. By integrating the diffusion equation the particle number density was found in terms of the particle number density at the base as shown in Eq. 2.

$$\frac{N}{N_b} = e^{-k'(1+sin\theta)};\ where,\ k' = \frac{T}{3.57u\sqrt{f}} \tag{2}$$

When a very reliable data of Jotaki et al. [11] giving concentration distribution was compared with theoretical $\frac{c}{c_b}$ predicted through Eq. 2, the agreement between the two (details shown by Chand et al [12]) for all $\frac{y}{D}$ appear to be excellent as could be seen through Table.2.

Table 2. CONCENTRATION VARIATION.

$\frac{y}{D}$	$\frac{c}{\bar{c}}$	$(\frac{c}{c_b})_{exp}$	$(\frac{c}{c_b})_{Th}$
1.000	0.342	0.148	0.148
0.865	0.440	0.190	0.192
0.710	0.600	0.260	0.258
0.565	0.755	0.328	0.340
0.440	1.050	0.456	0.432
0.300	1.300	0.564	0.564
0.140	1.735	0.753	0.765
0.000	2.305	1.000	1.000

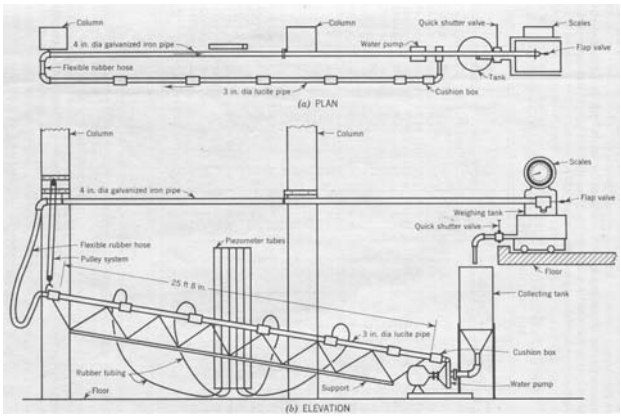

Figure 1. EXPERIMENTAL RIG OF SHIH- [13]

Table 3. COMPARED WITH TYPICAL DATA OF SHIH

S. No.	Slope	Re_{exp}	f_{sh}	f_{sj}	f_{bl}
(-)	ϑ	(-)	(-)	(-)	(-)
1	0.0	288467	.01713	.01717	.01365
2	0.0	311183	.01702	.01706	.01340
3	0.0	286059	.01719	.01719	.01368
6	8.73	315853	.01717	.01703	.01335
7	8.73	309463	.01723	.01706	.01341
9	8.73	294857	.01726	.01714	.01358
11	17.71	273858	.01728	.01726	.01383
16	17.71	297213	.01718	.01713	.01355
19	17.71	249948	.01740	.01742	.01415

2.3 Fluid- Wall Interaction

The need for the right form of correlation to connect friction factor with the pipe roughness parameter and Reynolds number becomes essential particularly when interference from end connections become too important to ignore.

As an example, the test-rig used by Shih [13] is shown in Fig. 1. After analysing his experimental set-up and establishing e/D (it was found to be $3.07X10^{-4}$) of the test section, when f_{sh} is compared with predicted values f_{sj}, the agreement between the two appear to be excellent as could be seen from Table 3. Further, the computed f_{bl} values are far from the experimental values f_{sh}.

Of the several friction factor equations available in the literature, Haaland equation [14] or Swamee & Jain equation [6] were found to be the right choice. The former is better as it could be used for even $\frac{e}{D} = 0$.

2.4 Solid-Fluid Pressure Along Flow Line

The three basic issues as listed above along with particle dynamics approach of Chand [9] helped in establishing a methodology to deal with solid-gas/ solid-liquid suspensions under a generalized flow field. For the contribution of pressure drop due to solids, the method proposed earlier [9] when used for sloped pipes yields Eq. 3.

$$\frac{du_p}{dx} = -\frac{g}{u_p}\left\{\frac{\rho_p - \rho_g}{\rho_p}\right\} Sin\vartheta(\hat{x}) - f_c\frac{g}{u_p} - f_0\frac{u_p}{D} + \frac{3\rho_g C_d}{4\rho_p d}\left\{\frac{u_g - u_p}{u_p}\right\}^2 \tag{3}$$

where,

$$f_0 = \frac{D}{12d} e_{eq} \left[1 - \left(\frac{D-2d}{D} \right)^2 e^{-\frac{2k'd}{D} cos(\vartheta)} \right] + \frac{D\lambda\rho_g}{6d(1-\lambda)\rho_s} e'_{eq} \quad (4)$$

and

$$f_c = 2\mu_1 d \left(\frac{D-d}{D^2} \right) \frac{H'}{H} cos\vartheta + \left(1 - \frac{\rho_g}{\rho_s} \right) sin\vartheta \quad (5)$$

Also,

$$H' = \int_{-\frac{\pi}{2}}^{\frac{\pi}{2}} \left\{ e^{-k(1+sin\theta)} \right\} (-sin\theta)(cos^2\theta) d\theta \quad (6)$$

and

$$H = \int_{-\frac{\pi}{2}}^{\frac{\pi}{2}} \left\{ e^{-k(1+sin\theta)} \right\} (cos^2\theta) d\theta \quad (7)$$

Ordinarily e_{eq}, e'_{eq} and μ being experimental constants are obtained by fitting the pressure distribution along pipe line after conducting experiment. The Least-Square-Distance Technique of Howell [15] when extended [16] for conveyance of materials like rock-phosphate and coal dust, the three experimental constants were found to be e_{eq} = 0.00165, e'_{eq} = 0.00172 and μ_1 = 0.84.

Table 4. RANGE OF EXPERIMENTAL VARIABLES

Variables	Rose-P	Rose-H	Shih-H
$u_{min}(\frac{m}{s})$	18.29	4.27	2.59
$u_{max}(\frac{m}{s})$	36.28	6.71	3.43
$W_{min}(\frac{kg}{s})$	0.04	0.50	0.41
$W_{max}(\frac{kg}{s})$	0.18	2.27	2.93
$Re_{min}(10^4)$	37.9	14.9	20.6
$C_{wmin}(\%)$	51.37	8.44	2.56
$Re_{max}(10^4)$	75.8	23.4	31.1
$C_{wmax}(\%)$	90.84	35.15	19.0
Pipe-$slope^0$	0	0	17.71

The works of Rose et al. [17], Saha [18] and Shih [13] with a wide variation in parameters (see Table 4) were of immense help in establishing the methodology. This part of the work is, in fact, a fairly exhaustive comparison of theoretical prediction with experimental data of many past researchers including those of Rose et al. [17], Saha [18] and Shih [13] and is left for presentation at a later stage. Only the prediction error bounds of some researchers are shown in Table 5 which confirms, to a great extent, the validity of systematic approach to the problem.

Table 5. % ERROR-THEORETICAL

	Rose-p	Rose-h	Shih-h
Max	6.62	18.99	4.08
Min	-5.65	-0.44	-1.92
Ave	0.33	8.24	1.01
RMS	2.63	9.91	1.76

2.5 Mixing Of Jets:- Boundary Layer Approach

The approach of Wang et al. [1] for boundary layer growth in pipe entry could be extended to predict the decay of the primary core and the growth of the secondary core in the mixing region of the jet pump.

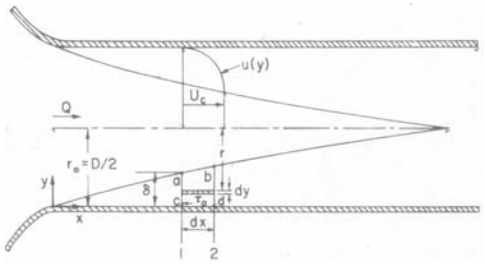

Figure 2. BONDARY LAYER IN PIPE ENTRY- Ref. Wang et al. [1]

Assuming the pumping action as visualized by Cunningham [2], the problem could be worked out for steady, incompressible and axi-symmetric flow. The details of the analysis is available in Ph.D. thesis of Raju [19] and [20]. A brief description of the method is presented now for the sake of better reading of the present paper.

Referring to Fig.3,

$$G = r_t - r_p; \;\; E = r_t - r_p + \delta; \;\; and \;\; \zeta = \frac{E}{r_t} \quad (8)$$

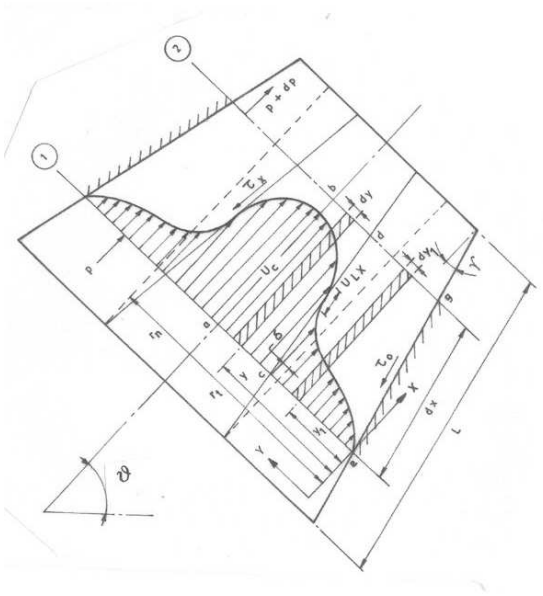

Figure 3. CONTROL VOLUME FOR MIXING OF JETS.

The velocity distribution in the primary jet is assumed to follow the power law equation. In the established flow region, the modified power law is as in Eq. 9.

$$u = u_c \left(\frac{y}{r_t}\right)^{\frac{1}{n}} \qquad E < y < r_t \tag{9}$$

To take care of the shear stress between the two jets, the slip velocity u_{LX}, could be calculated by using the continuity equation and can be expressed as:

$$u = u_{LX} + u_c \left(\frac{y}{r_t}\right)^{\frac{1}{n}} - u_{LX}\left(\frac{y}{E}\right)^{\frac{1}{n}} - u_{LX}\left(1-\frac{y}{E}\right)^{\frac{1}{n}} \qquad 0 < y \leq E \tag{10}$$

Similarly taking care of mass conservation, the average velocity of secondary fluid V_s and u_{LX} at a cross section turns out to be as shown in Eq.(s) 11 and 12 respectively.

$$V_s = \frac{V}{\zeta(2-\zeta)} - \frac{2nu_c}{(n+1)(2n+1)\zeta(2-\zeta)} \left[n - \{(2n+1)-(n+1)\zeta\}\,\zeta^{\left(1+\frac{1}{n}\right)}\right] \tag{11}$$

$$u_{LX} = \frac{n+1}{(n-1)\zeta(2-\zeta)} \left\{ \frac{2n^2 u_c}{(n+1)(2n+1)} - V \right\} \tag{12}$$

The shear stress at the junction of the two jets is given by Eq. 13, where C_{dx} is corresponding to Re_x obtained through Eq. 1 and $Re_x = \frac{u_{LX}\,(l_p - x)}{\nu}$.

$$\tau_x = \frac{K_1 \rho f_i V_s^2 (r_n - \delta)}{8 r_t} + \frac{\alpha K_2' \rho u_{LX}^2}{Re_x^{0.2}} + \frac{K_3}{2} C_{dx} \rho u_{LX}^2 \tag{13}$$

Conservation of mechanical energy: Considering conservation of mechanical energy, the energy equation can be written as in Eq. 14.

$$\begin{aligned} V\pi r_t^2 \left(\frac{dp}{dx} + \rho g \sin\vartheta\right) dx + 2\pi r_t V_s \left(\frac{f_i K_1 \rho V_s^2}{8}\right) dx \\ + \left(\frac{\alpha K_2' \rho u_{LX}^2}{Re_x^{0.2}}\right) 2\pi (r_t - E) u_{LX} dx \\ + \left(\frac{K_3 C_{dx} \rho}{2}\right) u_{LX}^2 \pi (r_n - \delta) u_{LX} d\delta \\ + \frac{d}{dx} \int_0^{r_t} 2\pi \rho (r_t - y) u^3 dy dx = 0 \end{aligned} \tag{14}$$

Equation of motion for secondary and primary jets: After incorporating the mass flow rate of the fluid that enters from the element 'abcd' through 'cd' into the element 'cdeg', the rate of change of momentum turns out to be as in Eq. 15 for the secondary jet and Eq.16 for the primary jet.

$$\begin{aligned} -\pi \left[r_t^2 - (r_n - \delta)^2\right] \left(\frac{dp}{dx} + \rho g \sin\vartheta\right) dx - 2\pi r_t \tau_0 dx \\ + (u_d - u_{LX}) \frac{d}{dx} \left[\int_0^E \rho 2\pi (r_t - y_1) u dy_1\right] dx + F_{dp} \\ - \frac{d}{dx} \left[\int_0^E \rho 2\pi (r_t - y_1) u^2 dy_1 dx\right] + 2\pi (r_n - \delta) \tau_x dx = 0 \end{aligned} \tag{15}$$

Where F_{dp} is the drag force due to the presence of particles in the secondary fluid.

$$-\pi (r_n - \delta)^2 \left(\frac{dp}{dx} + \rho g \sin\vartheta\right) dx - 2\pi (r_n - \delta) \tau_x dx$$

$$-\frac{d}{dx}\int_E^{r_t} \rho 2\pi (r_t - y)\, u^2 dy dx$$
$$-u_\delta \frac{d}{dx}\int_E^{r_t} \rho 2\pi (r_t - y)\, u dy dx = 0 \qquad (16)$$

Next the set of first order differential equations Eq.(s) 14, 15 and 16 was solved by the fourth order Runge-Kutta method to obtain the values p, u_c and ζ at a section for given initial conditions. The mixing phenomenon will continue till the primary core decays completely, dissipating its energy and momentum to the secondary jet. A typical comparison of the theoretical prediction using experimental data of Sanger [21] and [22] when the nozzle is placed just at the throat entry ($\frac{s}{d_t}$ =0) is shown in Fig. 4.

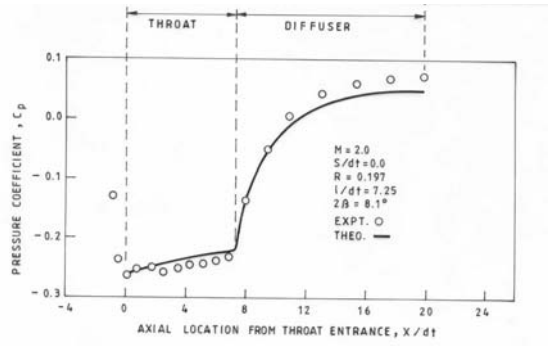

Figure 4. RESULTS COMPARED WITH SANGER'S DATA

In Fig. 4, the pressure coefficient at a section is defined in the non-dimensional form as in Eq. 17.

$$c_p = \frac{p_x - p_a}{\rho \frac{V_n^2}{2}} \qquad (17)$$

3 SOLID HANDLING JET PUMP

Having established a methodology based on strong footing, we now limit our study mainly to diffuser and transport regions of the jet pump assuming that the mixing process between the phases is completed in the throat itself. Taking a generalized duct having area A, fluid velocity u, solid velocity u_p and pressure p at a section x changing to A+dA, u+du, $u_p + du_p$ and p+dp respectively at section at x+dx and making use of geometrical variation in A, conservation of mass, and momentum of the two phases, and thus forming a set of simultaneous differential equations in a manner as it was done in one of our previous works [23]. They were solved by using the fourth order Runge-Kutta method to obtain the values of A, u, u_p and p at a section for the given initial conditions. In order to check the validity of the equations developed for different cases, a software package was developed to predict the pressure distribution along a flow line which were compared with the experimental data generated on experimental setup shown in Fig. 5.

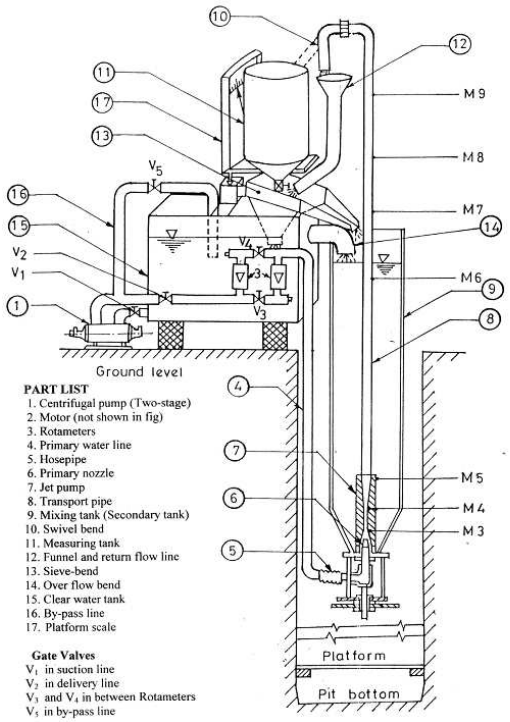

Figure 5. SCHEMATIC VIEW -EXPERIMENTAL RIG

4 EXPERIMENTAL PROGRAM

The jet pump and the duct connecting the main setup consisted of acrylic material. The transport pipe marked as (8) in Fig. 5 was of 25.4 mm diameter having wall thickness of 3 mm. The three primary nozzles had sharp outlets of 6, 7 and 8 mm respectively. Major specifications of jet pumps were-(i) Diameter of throat, $d_t = 12.7mm$,(ii) Length of throat, $l_t = 63.5mm$ and (iii) Diffuser angle = 6.5^o. For pressure measurements, pressure taps marked as M3 through M9 in the Figure were located at 0.0, 0.0635, 0.1752, 1.5296, 2.3872, 2.6872, and 2.9872 m respectively. Sand of three different mean sizes (232, 420 and 684 μm) were conveyed at several flow velocities ranging from 3.20 m/s to 0.92 m/s.

5 RESULTS AND DISCUSSIONS

Using a software package developed for the purpose, the variation of pressure along the flow line starting from nozzle exit to any station on the down-stream side could be found. The package is capable of taking care of the so-called unbalanced situation like particle moving at higher velocity than the fluid. In general the pressure variation along flow line for few typical flow parameters like sand of mean size 232 μm are as shown in Fig.(s) 6, 7, and 8.

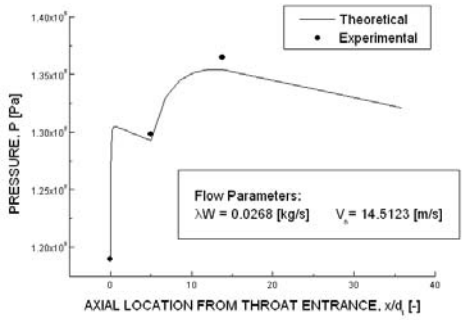

Figure 6. PRESSURE -THROAT ENTRY ONWARD.

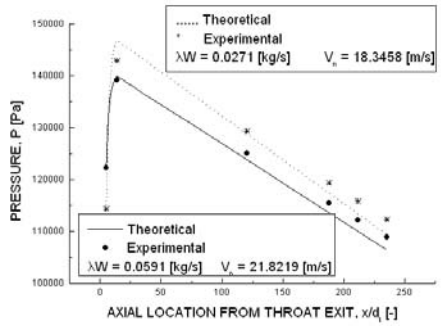

Figure 7. PRESSURE IN DIFFUSER ONWARD.

While proceeding for integration along flow lines in the three figures the integration begins from throat entrance, throat and diffuser exit respectively. Along with the theoretical curves, experimental points have been shown for all the 7 points. The agreement between the theoretical points and the experimental values appear to be good particularly when integration begins from throat exit (Fig. 7) and diffuser exit (Fig. 8). The pressure built-up in the diffuser region could be clearly seen. When the mixture passes through the transport region, there is a continuous pressure loss almost at constant rate as seen through Fig.8.

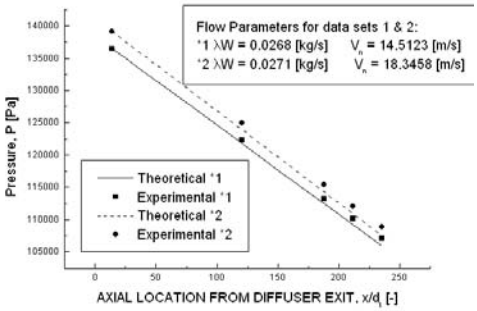

Figure 8. PRESSURE- DIFFUSER EXIT ONWARD

Interference due to end connectors : As stated earlier, the upstream and downstream elements interact with the main element and leave a mark on it. The interference effects due to diffuser on the one hand and end connectors at the other end of the transport pipe are considered here to elaborate the interference effects of the two.

The fluid phase and the solid phase play their own role in the interference process. The role played by solid phase results in weak or strong interference depending on whether the solid phase velocity dictated by Eq. 3 results in a velocity smaller or larger than the one under steady state and established flow conditions.

As an example, when the solids have to be picked up from the secondary section of the pump and has to pass through the mixing region, weak interference is expected. But when the solid phase has to get into transport region from the diffuser region, strong interference is expected. The degree of the interference coefficient depends on the difference in the actual velocity of the solid phase from its velocity in the established flow region. This has to be established only at the input point from where the integration begins. Next, the output parameters of one section becomes the input parameter of the next section.

For interference effect due to the fluid phase, the transport pipe is assumed to have three -(i) developing (ii) developed and (iii) reformed sections. It is assumed that in the developing region, the value of n in power law and friction factor are highest at the entry of the duct and then decreases exponentially to the established flow values. Also on the downstream side the reverse happen. This requires two interference coefficients -one (K_4) for the upstream, another (K_6) for the downstream regions and yet another (K_5) to dictate the rate at which n and f change from their maximum values to those in the established region of the duct. The effect of the three coefficients - (K_4) through (K_6) on

pressure variation along flow line, when integration begins from same initial pressure conditions as at the exit of the diffuser, is presented in Fig.(s) 9 - 11 respectively.

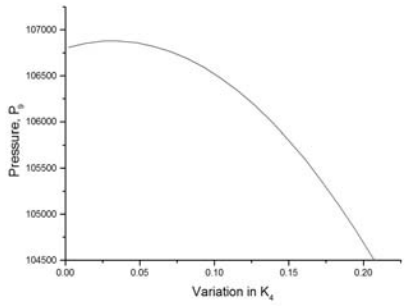

Figure 9. EFFECT OF COEFFICIENT K_4.

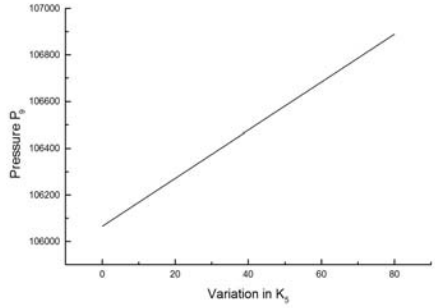

Figure 10. EFFECT OF COEFFICIENT K_5.

Job done through the software after introducing correct interference coefficients $K_4 - K_6$ resulted in yielding close agreement of pressure distribution as could be seen through Fig. 12. The error bounds at 4 locations (M-6 through M-9) shown in Table 6 also confirm the goodness of the fit. This was only expected because we systematically considered the five essential aspects as stated in section 2 of this paper. Also we took care of the interference coefficients $K_4 - K_6$ under actual condition of the transport pipe marked as (8) in the test rig shown in Fig. 5. This resulted in having developing and reformed sections of respectively 0.02 and 0.2 times the transport pipe length which too appear to be fairly reasonable.

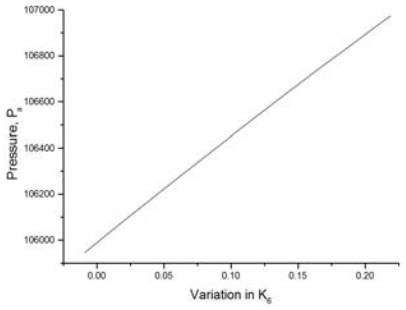

Figure 11. EFFECT OF COEFFICIENT K_6.

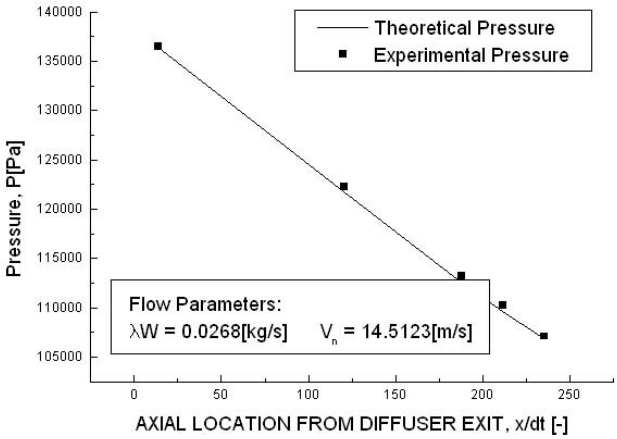

Figure 12. PRESSURE-DIFFUSER EXIT TO ONWARD.

Table 6. % ERROR AFTER ESTABLISHING K4-K6.

P-At	Max	Min	Ave	RMS
M-6	1.58	0.00	0.06	0.26
M-7	2.10	0.00	0.08	0.35
M-8	0.81	0.00	0.03	0.13
M-9	0.00	-0.51	-0.02	0.10

6 CONCLUSIONS

For a general sample, it is recommended to first characterize the sample for its ψ value by conducting experiment determining the drag coefficient versus Reynolds number plot for the sample.

When as a typical case Shih experimental data was analysed, very high value of f was found. In our view, it must be due to several couplings, and pressure taps between the test section

and also due to subtle interference from end connectors. Further, the manner in which the test duct is supported, also contributes towards e/D value. It is recommended to have experimental data generated on a model test pipe to obtain the equivalent roughness parameter for the particular portion of the pipe. The same equivalent roughness parameter can be used for extrapolation for the prototype.

We thus have an approach which can take care of interference effects and simulate pressure distribution along the flow line in a systematic manner. It is advisable to begin simulation from one end of the system and proceeding to next element until the complete system has been covered. While doing that the parameters at the end conditions of a section have to be the input parameters of the next section.

The work was further extended to include the five basic issues listed earlier along with Boundary Layer approach to mixing of two jets mainly in the throat region of the jet pump. This of-course forms our program for coming research work.

7 ACKNOWLEDGEMENT

The authors would like to thank Mr A K Datta [24], for initiating this work, Dr. D Ranga Raju [19] for working further and Mr. C R Hansda for his sincere help in setting up excellent test rig.

REFERENCES

[1] Wang, J. S., and Tullis, J. P., 1974, "Turbulent Flow in the Entry Region of a Rough Pipe", Trans. of the ASME, Journal of Fluids Engineering, vol. 96, No. 1, pp. 62-68.

[2] Cunningham, R. G., 1975, "Liquid jet pump modelling:- Effects of axial dimensions on Theory-Experimental Agreement", 2nd Symposium on Jet Pumps and Ejectors and Gas lift Techniques, BHRA, Paper F1, pp. 1-15.

[3] Reddy, Y. R. and Kar, S., 1968, "Theory and performance of water jet pumps", Proc. ASCE, J. Hyd. Div., Vol.94, No. HY5, pp.1261-1281.

[4] Ng, K. L., 1989, "Coal Unloading System Using a Slurry System", Bulk Solids Handling, vol. 9, No. 3, pp. 281-287.

[5] Idelchick, I. E., 1991, "Fluid Dynamics of Industrial Equipment", Hemisphere Pub. Corp., New York.

[6] Miller, D. S., 1971, "Internal Flow: A Guide to Losses in Pipe and Duct Systems", BHRA, Bedford, U.K., pp.329.

[7] Brown, G. G., 1950, "Unit Operations", John Wiley and Sons Inc., New York.

[8] Chand P., Reddy Y. K., Saha A. C., Chand B. R., 2001, "On Drag Coefficient of Non-Spherical Particles", Powder Handling and Processing, Vol-13, No.-3, pp 289-291.

[9] Chand, P., 1971, "Response of Particles Under Pneumatic Conveyance", Proc., PNEUMOTRANSPORT 1, BHRA, UK, Paper- B6, pp. 69-91.

[10] Taylor, S. G., 1954, "The Dispersion of Matter in Turbulent Flow Through a Pipe", Proc. Royal Soc. Of London, 223, Series A, pp. 446.

[11] Jotaki, T., and Tomita, Y., 1971, "Solids Velocities and Pressure Drops in a Horizontal Pneumatic Conveying System", Proc., PNEUMOTRANSPORT-1, BHRA, UK, Paper B3, pp 33-43.

[12] Chand P., Reddy Y. K., Saha A. C., 2001, "On solid-Gas diffusion Coefficient", Powder Handling and Processing, Vol-13, No.-4, pp. 353-356

[13] Shih, C. C. S., 1964, "Hydraulic transport of solids in a sloped pipe", J. of the PIPELINE DIVISION, Proc. of the ASCE, Vol.90, PL.2, pp. 1-14.

[14] Haaland, S. E., 1983, "Simple and Explicit Formulas for Friction factor in Turbulent Flow", Transaction ASME, Journal of Fluids Engg., Vol. 105, pp. 89.

[15] Howell, J. G., "A Least Square Distance Curve Fitting Technique", NASA TN D-6374.

[16] Chand P., 1989, "Design Parameters for Pneumatic Conveying of Rock Phosphate and Coal Dust", Report submitted to Projects and Development of India Ltd., Govt. of India Undertaking, Mech. Engg. Dept., IIT Kharagpur, India.

[17] Rose, H. E., and Duckworth, R. A., 1969, "Transport of Solid Particles in Liquids and Gases", The Engineer, vol. 14, No. 21, pp.1-16.

[18] Saha, A. C., 1997, "Wear Modelling of 90^0 Bend Conveying Air-Solid Mixture", Ph.D. Thesis, Mechanical Engg. Dept., IIT Kharagpur, India.

[19] Raju, D. R., 1988, "Dynamics of Jet Pumps with specific reference to hydraulic transportation of solids", Ph.D. Thesis, IIT Kharagpur, India.

[20] Reddy, Y. K., Raju, D. R., Chand P., 1990, "Computer Aided Performance Evaluation of Jet Pumps", Journal of Institution of Engineers (India), vol. 71, part ME 6, pp. 151-157.

[21] Sanger N. L., 1968, "Noncavitating performance of two low area ratio water jet pumps having throat lengths to diameter ratio of 7.25, 5.66, 3.54 ", NASA Report TN D - 4445. 4759 and 5095.

[22] Sanger, N. L., 1970, "An experimental investigation of several low area ratio water jet pumps", Trans. of the ASME -J. of Basic Engng, Vol. 92, No.1, pp. 11-20.

[23] Chand, P., 1973, "A Theoretical Model of the Pneumatic Conveying-Drying System", Proc.,2nd Internatial Conference on Pneumatic Transport of Solids in Pipies, PNEUMOTRANSPORT 2, BHRA, UK, Paper C2, pp. 15-27.

[24] Datta, A. K., 1984, "A Comparative Study of AIR-LIFT AND WATER-LIFT JET PUMPS-Applicable to Deep Sea Mining", M. Tech Thesis, IIT Kharagpur, India.